Topological Phase Transitions in Antiferromagnet and Topological Insulator Trilayer Structure

Luyan Yu†, Gen Yin‡, Qinglin He‡ and Kang L. Wang‡

†Kuang Yaming Department, Nanjing University, China

‡Department of Electrical Engineering, University of Los Angeles, California

yuluyan@g.ucla.edu

Abstract

In this project, we theoretically explain the asymmetric longitudinal resistance in the magneto-resistance measurement of antiferromagnet and topological insulator trilayer structure (AFM/TI/AFM). In this theory, this phenomenon is attributed to a series of topological phase transitions induced by double switching of interface magnetization.

Background

In recent years, topological matter and topological phase have been a popular area in the study of condensed matter physics. As we all know, matter can exist in different states, whose internal structures are characterized by order parameters. Lev Davidovich Landau's theory based on symmetry was believed to be a complete theory that could be used to understand any phenomenon of phase transition.

However, with the development of cryogenics, experiments can be done in an extremely low temperature, where quantum behavior starts to dominate. A new class of orders, the topological orders, has emerged. Topological order reveals a system's quantum behavior in zero temperature. A famous and widely-used topological order is the Chern Number, which intuitively counts the number of edge states of a system.

Experiments

The following figure is the experimental results of SQUID and transport measurements of CrSb/In_2Se_3 bilayer, CrSb/TI bilayer and CrSb/TI/CrSb trilayer.

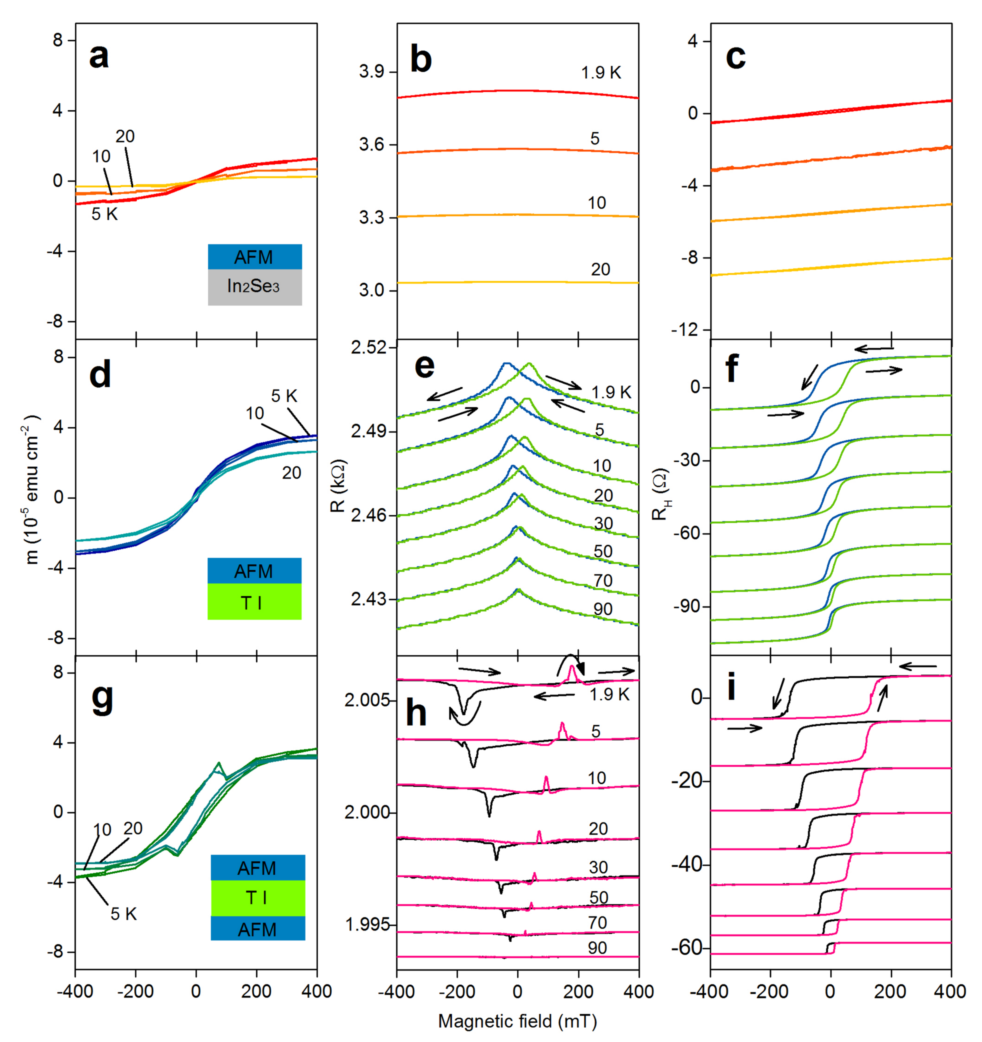

Figure 1: SQUID and transport results for CrSb thin films. (a)M-H measurement results of a 12-nm CrSb thin film grown on a buffer layer of In_2Se_3. (b, c) The longitudinal and the Hall resistance measured from a 1mm × 2mm Hall bar fabricated from the thin film corresponding to (a). (d-f) SQUID and transport measurement results on a CrSb/TI bilayer. (g-i)SQUID and transport results on a CrSb/TI/CrSb trilayer.

Modeling

We starts with the well-known TI thin film Hamiltonian[2], as is the blue part of the following equation:

$$H = \begin{pmatrix} \frac{\Delta}{2} - Bk^2 & i\gamma k_- & V & 0 \\ -i\gamma k_+ & -\frac{\Delta}{2} + Bk^2 & 0 & V \\ V & 0 & -\frac{\Delta}{2} + Bk^2 & i\gamma k_- \\ 0 & V & -i\gamma k_+ & \frac{\Delta}{2} - Bk^2 \end{pmatrix} + H_H, \quad (1)$$

where $k_\pm = k_x \pm ik_y$ and $k^2 = k_x^2 + k_y^2$; $B > 0$ is the parabolic massive component, Δ is the hybridization gap and V is the surface-to-surface potential drop.

A Hunds-rule coupling term H_H is added to account for the effect of two different interfaces:

$$H_H = -J_H \begin{pmatrix} \boldsymbol{S}_T \cdot \boldsymbol{\sigma} & 0 \\ 0 & \boldsymbol{S}_B \cdot \boldsymbol{\sigma} \end{pmatrix} \quad (2)$$

where J_H denotes the interfacial Hunds-rule coupling induced by the wave function overlap.

Hunds-rule coupling term adds massive terms to the total Hamiltonian, such that the reversal of $\boldsymbol{S}_{T,B}$ changes the band order, inducing topological transitions. Assuming a thick enough TI thin film, $\Delta = V = 0$, and the total Chern number is the sum of the Chern numbers given by the top and bottom surfaces: $C = C_T + C_B$.

Schematically, the process of magnetization double switching can be described in the following figure.

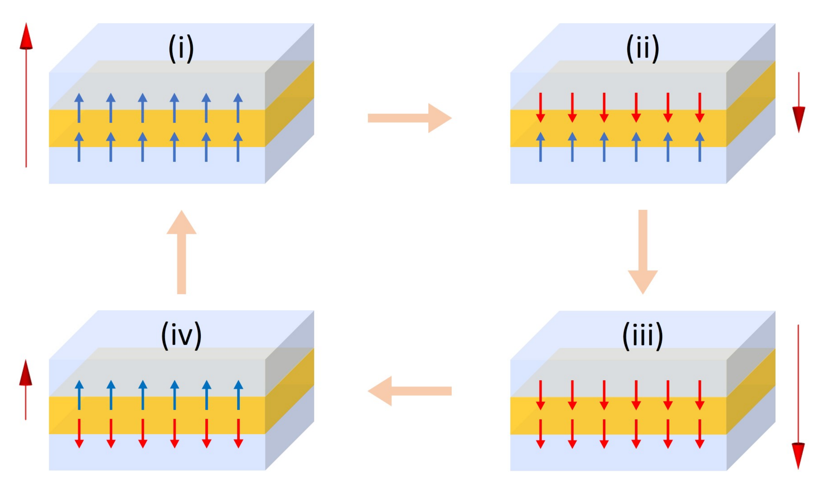

Figure 2: Magnetization double switching process. (i) In the beginning, because of the existence of relatively strong magnetic field, both interfaces have their magnetization pointing upwards. (ii) When the external magnetic field changes direction and gradually increases, one of the interface flips its magnetization first (top in the figure). (iii) With the increasing of reversed magnetic field, the other interface flips its magnetization. (iv) The external magnetic field changes the direction again and the top interface switches its magnetization.

Methods

Tight Binding Approximation

Replace momentum operators with finite difference on the lattice grid:

$$k_x \to -i\frac{\partial}{\partial x} \to -i\frac{\Delta}{\Delta x}, \quad k_y \to -i\frac{\partial}{\partial y} \to -i\frac{\Delta}{\Delta y}. \quad (3)$$

Bra-ket inner product can be written into difference format:

$$\langle i_x, i_y | k_x | j_x, j_y \rangle \to -i \langle i_x, i_y | \frac{|j_x + 1, j_y\rangle - |j_x - 1, j_y\rangle}{2\Delta x}.$$

After discretization, we will have an on-site term ϵ standing for the on-site energy, and two hopping terms t_x and t_y representing nearest neighbor hopping along x and y directions.

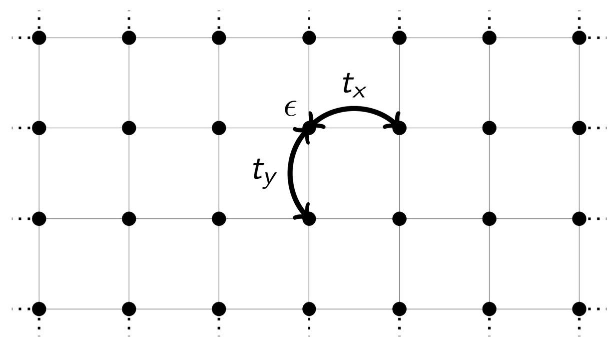

Figure 3: Discretized device lattice grid with on-site term ϵ and hopping term along x, y direction t_x, t_y.

Non-equilibrium Green's Function

NEGF formalism is a framework for the quantum mechanical simulation of nano-scale device[1]. Some of the advantages listed below enable us to investigate this particular problem.

- Handle strong external field non-perturbatively;
- Take into account the effect of contact in terms of self energy;

$$\begin{cases} G^R = [\epsilon - H_D - \sum_i \Sigma_i]^{-1} \\ \Gamma_i = i(\Sigma_i - \Sigma_i^\dagger) \end{cases} \to T_{ij} = \mathrm{Tr}[\Gamma_i G_{ij}^R \Gamma_j G_{ij}^{R\dagger}] \quad (4)$$

Finite Temperature

Because the experiment was done in 1.9K, finite temperature will smear out the exact Fermi level. To account for this effect, the following integral is used to calculate the current:

$$\boldsymbol{I} = \frac{e}{h}\left[\int \left(-\frac{\partial f_0}{\partial \epsilon}\right) \boldsymbol{T}(\epsilon) \mathrm{d}\epsilon\right] \delta\boldsymbol{\mu}, \quad (5)$$

where $\boldsymbol{I} = (I_1, I_2, \cdots, I_6)^T$ denotes the current at different terminals, $\delta\boldsymbol{\mu} = (\delta\mu_1, \delta\mu_2, \cdots, \delta\mu_6)^T$ denotes the chemical potential shift ($\delta\mu_i = \mu_i - \epsilon_F$), and $\boldsymbol{T}(\epsilon)$ is the transmission coefficient matrices of different energies.

Results

NEGF calculation indicates the existence of edge states in the six-terminal Hall bar geometry.

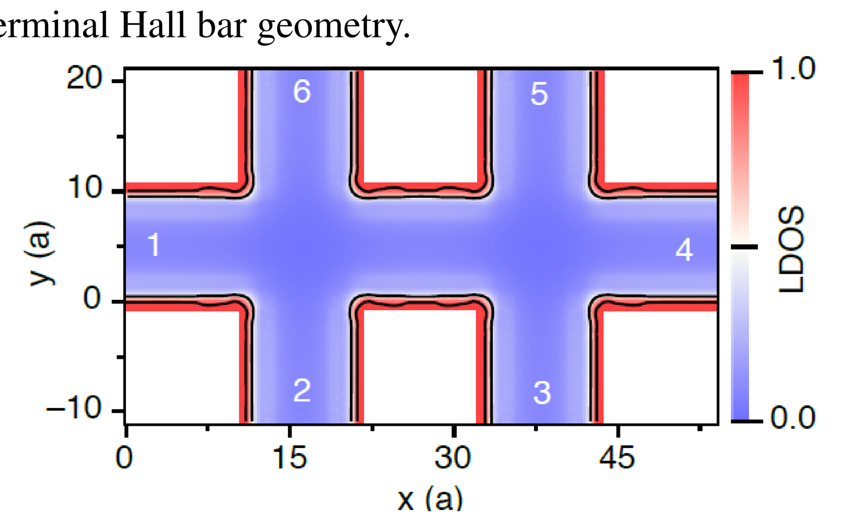

Figure 4: Local density of state (LDOS) on the hall bar geometry calculated using NEGF. High LDOS on the edge colored by red is indicated in the figure.

Finite temperature leads to the smearing out of quantized resistance.

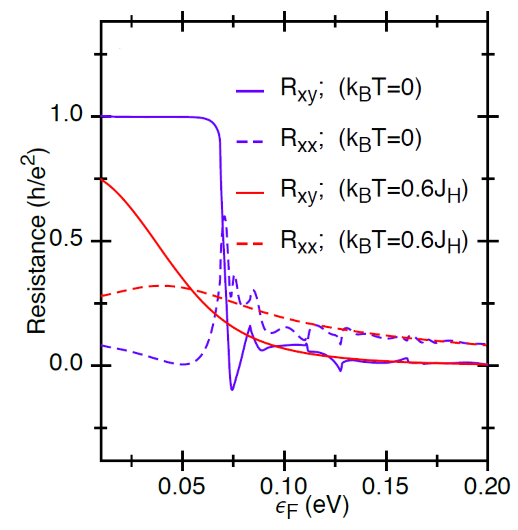

Figure 5: Longitudinal and transverse resistance under Zero temperature and finite temperature.

Theoretical calculations are consistent with experimental results: at all Fermi energies, the longitudinal resistance of up-up and down-down magnetization configurations are between that of up-down and down-up configurations.

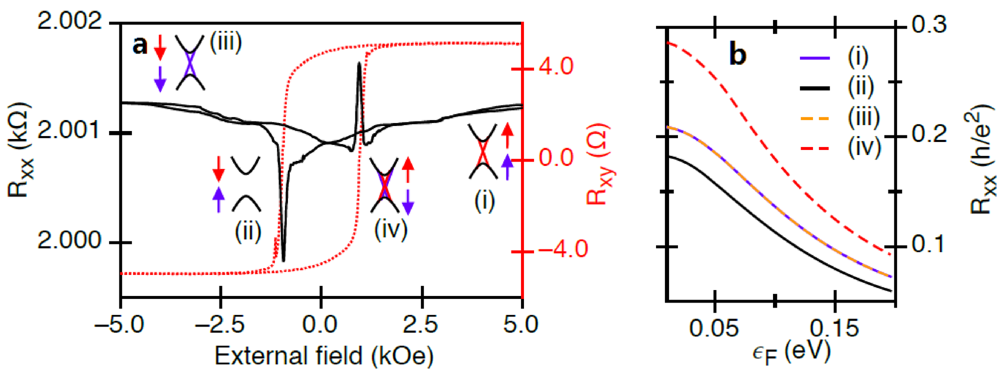

Figure 6: (a)Experimental results of longitudinal resistance in the process of external magnetic field scanning. The four stages (i),(ii),(iii),(iv) corresponds those in Fig. 2. (b)Theoretical calculations of longitudinal resistance using NEGF.

When $\boldsymbol{S}_T$ and $\boldsymbol{S}_B$ are parallel, only one surface is topologically non-trivial, such that $C = \pm 1$. The dispersions of these modes are shown as the colored linear bands in Fig. 7(a) and (c). As shown in Fig. 7(b), when $\boldsymbol{S}_T$ is down and $\boldsymbol{S}_B$ is up, $C_T = -1$ and $C_B = 1$, the edge modes show up, with 2-fold degeneracy (Fig. 7(b)). However, in the case when $\boldsymbol{S}_T$ is up and $\boldsymbol{S}_B$ is down, $C_T = C_B = 0$ and the exchange band gap becomes trivial.

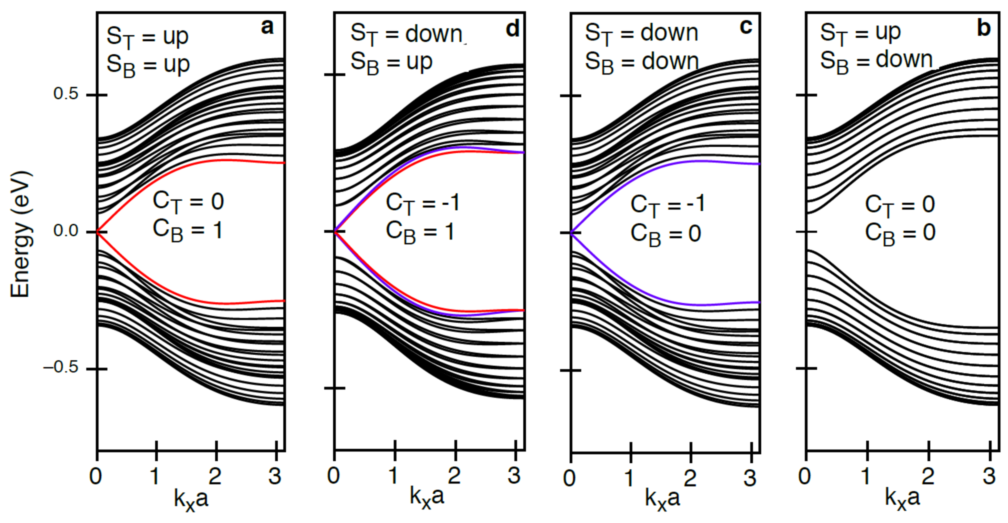

Figure 7: Band structure of each topological phase

Conclusions

In conclusion, proximity effect between AFM and TI is confirmed by both MR measurement results and NEGF calculation. The existence of proximity effect can lead to the topological phase transition between induced by magnetization double switching.

Acknowledgment

The author would like to thank to Prof. Kang L. Wang for providing such an opportunity to join his group, Gen Yin for his continuous guidance on projects, Qinglin He for providing the breakthrough experimental data, all CSST directors and coordinators for their thoughtful organizations of CSST program, all CSST students for the happiness that they bring.

References

[1] S Datta. Nanoscale device modeling: the Green's function method. *Superlattices and microstructures*, 2000.

[2] H Z Lu, A Zhao, and S Q Shen. Quantum transport in magnetic topological insulator thin films. *Physical review letters*, 2013.